Application of the method of multiple scales for nonlinear vibration analysis of mechanical systems with dry and lubricated clearance joints

Saeed Ebrahimi [*], **Esmaeil Salahshoor**, **Mohsen Maasoomi**

Faculty of Mechanical Engineering, Yazd University, Yazd, Iran

ARTICLE INFO

ABSTRACT

In this study, the method of multiple scales is used to perform a nonlinear vibration analysis of a mechanical system in two cases; with dry and lubricated clearance joints. In the dry contact case, the Lankarani-Nikravesh model is used to represent the contact force between the joined bodies. The surface elasticity is modeled as a nonlinear spring-damper element. Primary resonance is discussed and the effect of the clearance size and coefficient of restitution on the frequency response is presented. Then, a frequency analysis is done using the Fast Fourier Transform. A comparison between the Lankarani-Nikravesh and Hunt-Crossly contact force models is made. The results obtained numerically and analytically had an acceptable agreement. It is observed that decreasing the clearance size changes the frequency response in the primary resonance analysis. Furthermore, Hunt-Crossly contact force model showed a slightly more dissipative effect on the response. In the lubricated joint case, a linear spring and a nonlinear damper based on the Reynolds equation developed for Sommerfeld's boundary conditions are used to model the lubricant behavior. It is shown that only the fluid stiffness has influence on the amplitude of the steady state response and the fluid does not make any effect on the response frequencies after the transient response vanishes. The steady state response frequency for both dry and lubricated cases depends on the linear natural frequency corresponding to the pendulum oscillation. In the primary resonance analysis, increasing the dynamic lubricant viscosity decreases the amplitude in the vicinity of the linear natural frequency as expected.

[*] Corresponding author.
E-mail address(es): ebrahimi@yazd.ac.ir (S. Ebrahimi), esalahshoor@stu.yazd.ac.ir (E. Salahshoor), m.masoomi@stu.yazd.ac.ir (M. Masoomi).

1. Introduction

In multibody systems, kinematic joints are generally assumed to be without clearance. However, in real mechanical joints, there is always some clearance between the journal and the bearing. This clearance is necessary in the assembly of the mechanical system because it allows the connected bodies to move relative to each other. The clearance exists due to machining tolerances, wear, material deformations and imperfections and it can deteriorate the performance of the mechanism regarding its precision and vibrational behavior. The clearance can lead to some deficiencies in the efficient and precise performance of mechanical systems. The influence of clearance on the dynamic response of the mechanical systems has been greatly investigated in the literature. However, nonlinear vibrational analysis of such systems is less presented. Numerical solution is the most common method for solving problems including clearance. Analytical solution can also be used to provide deeper insight into the system behavior by inspecting the effect of a certain parameter on the dynamic response.

Clearance has attracted a vast investigation by researchers. Three major types of clearance model can be found in the literature, namely, the massless link approach, the spring–damper approach and the momentum exchange approach. In the momentum exchange approach, the clearance is modeled through considering two colliding bodies and the dynamic behavior of the system is controlled by the impact-contact force between them. The impacts in the clearance joint make high contact force and consequently high acceleration. This model is more realistic than the two other approaches due to considering the contact forces as a function of surface elasticity in addition to taking into account the energy dissipation during impact [1]. Dubowsky and Freudenstein [2] used an impact pair model for the joint clearance. In their model, the contact surface was considered as a spring-damper element which was apart from the other surface within the clearance size. Rhee and Akay [3] studied the response of a four-bar linkage with a clearance joint and revealed that there is a nonlinear dependence on both the clearance size and the coefficient of friction between the journal and the bearing. Ravn [4] investigated a slider-crank mechanism with a clearance in the joint between the coupler and the slider. The continuous contact force model in which the contact force was a function of the amount of penetration between the journal and the bearing was used. Schwab et al. [5] compared several continuous contact force models with an impact model. It was realized that the compliance of the links or lubrication of the joint makes the peak values of the contact forces smoother. Flores et al. [6] studied the clearance in a multibody system taking lubrication into account. The compressive force exerted by the lubricant, when the journal and the bearing are not in contact, was considered in the equations of motion. Spatial flexible multibody systems was investigated by Tian et al. [7], taking the influences of the clearances and lubrication in the system spherical joints into account. Tian et al. [8] introduced a method to model and study the flexible spatial multibody systems with clearance cylindrical joints. For more information on the lubricated clearance joint, the reader is referred to [9, 10]. Brutti et al. [11] modeled a 3D clearance revolute joint with computer which could be implemented in multibody dynamic solvers. The dynamic behavior of a planar flexible slider-crank mechanism with clearance was investigated by Khemili and Romdhane [12]. The model was created in the ADAMS software and experimental investigations were carried out. It was revealed that the coupler flexibility acts as a suspension for the linkage in the presence of clearance. A method was introduced by Mukras et al. [13] to investigate the planar multibody systems in which wear appears at one or more revolute joints. The influence of the clearance on the slider acceleration, contact force and power consumption

was studied in a multi-objective optimization problem introduced by Zhang et al. [14]. Some other investigations on the optimization of mechanical systems with clearance can be found in [15-17]. Due to high nonlinearity of the clearance joint behavior, some effort has been dedicated to the investigation of the chaos and bifurcation in multibody systems with clearance (see [18, 19]).

Although there is a great amount of research on modeling the clearance and investigating its influence on the dynamic response of the multibody systems, few research works consider the effect of clearance and surface elasticity on the vibrational behavior. Vaidya and Padole [20] considered a four-bar linkage with clearance. They modeled the bearing stiffness as a linear and torsional spring and added this stiffness to the assembled stiffness matrix to find out the effect of joint flexibility on natural frequencies. Erkaya [21] investigated the effect of clearance on the vibration of the bearing for a slider-crank mechanism. He designed a neural network for different clearance sizes and velocities. He obtained the data from three accelerometers to recognize the system vibration. The network inputs were time, clearance size, velocity and the material of the mechanism and its outputs were the three accelerometers' data. Yang et al. [22] studied the vibrational modes of a cantilever beam with a block placed on it including clearance. Furthermore, very limited attention has been devoted to qualitative analysis of the effect of surface elasticity in clearance joints on the dynamic response and vibrational behavior of mechanical systems. The multiple scales method can be used to solve the equations of motion analytically. Although this method has some limitations to be used in solving more complex equations of motion, the closed-form solution, if obtained, provides a deeper insight into system behavior [23].

As a new study, in this paper, the method of multiple scales is used to perform a nonlinear vibrational analysis of a sliding pendulum including clearance with and without lubrication. Analytical solution can be used to give deeper insight into the system behavior understanding the effect of a certain parameter on the dynamic response. The momentum exchange approach is used to model the clearance. In the dry joint case, the Lankarani-Nikravesh contact force model is employed to model the contact force between the joined bodies. The surface elasticity is modeled as a nonlinear spring and a nonlinear damper which are described by the above mentioned contact force model. The nonlinear spring shows the Hertz contact law while the nonlinear damper represents the energy dissipation during contact through using the Lankarani-Nikravesh contact force model. Primary resonance is explained and the influence of the bearing radius (clearance size) and the restitution coefficient on the frequency response is shown. Then, a frequency analysis is performed using the Fast Fourier Transform. A comparison between the Lankarani-Nikravesh and Hunt-Crossly contact force models is made. In the lubricated joint case, a linear spring and a nonlinear damper based on the Reynolds equation developed for Sommerfeld's boundary conditions are used to model the lubricant behavior. The numerical and analytical responses are compared and the effect of the dynamic lubricant viscosity on the system's frequency response in primary resonance analysis is investigated.

2. Sliding pendulum with dry and lubricated clearance joints

In this study, a pendulum attached to a slider moving with a constant velocity is modeled. A clearance is supposed to exist in the joint between the slider and the guide. The contact is

modeled with a nonlinear spring based on the Hertzian theory and a nonlinear damper proposed by Lankarani and Nikravesh [1]. The real system and its simplified model are shown in Fig. 1.
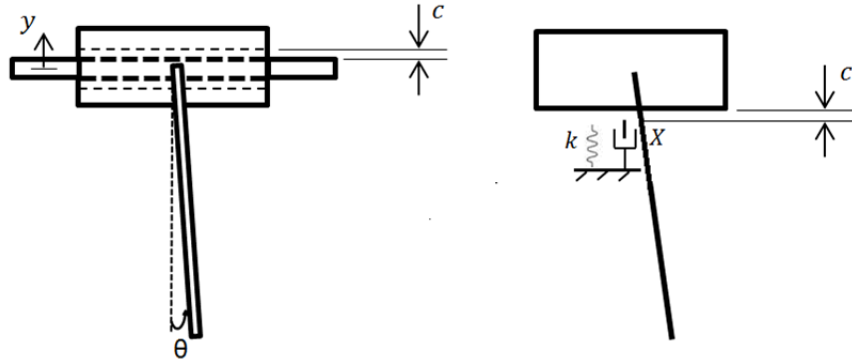

Fig.1. Model of the clearance between the slider and the guide

The motion of the slider perpendicular to the plane, outwards or inwards, is not considered. In addition, it is assumed that the angle between the contact force and the vertical line is small enough to consider the contact force as vertical. Lack of force in the tangential direction may be a good justification for such assumption.

2.1. Equations of motion

The equations of motion are derived using the generalized Newton's second law of motion as follows:

$$\left(m+m_1\right)\ddot{y}+m\frac{L}{2}\sin(\theta)\ddot{\theta}=F_N-\left(m+m_1\right)g-m\frac{L}{2}\dot{\theta}^2\cos(\theta) \tag{1}$$

$$m\frac{L}{2}\sin(\theta)\ddot{y}+m\frac{L^2}{3}\ddot{\theta}=-mg\frac{L}{2}\sin(\theta) \tag{2}$$

where m is the pendulum mass, m_1 is the slider mass, L is the pendulum length, θ is the angular position of the pendulum and y is the vertical position of the slider with respect to the center of the guide line.

It is noteworthy to mention that when the journal and the bearing are not in contact, the contact force is set to be zero. This could be found by calculating the relative penetration as:

$$\delta=\left|y\right|-c \tag{3}$$

where c is the clearance size. The contact force in the equations of motion is omitted if δ is negative since there is no contact between the journal and the bearing. When the relative penetration is positive, the contact force is calculated and is incorporated into the equations.

2.2. Contact force model

The Hertzian theory is the basis of many contact force models which introduce terms to represent the energy dissipation during the contact-impact phenomenon. Pure elastic contact force models cannot consider the energy dissipation during the contact process. Hence, more developed

contact force models must be used to take the energy loss into account. Several researchers improved the Hertz contact law to consider energy dissipation in the form of internal damping. The models suggested by Hunt and Crossley (1975), Lankarani and Nikravesh (1990), Gonthier et al. (2004), Flores et al. (2011) and Gharib and Hurmuzlu (2012) are instances of models that are employed to study multibody systems having contacts [24]. In this research, the Lankarani-Nikravesh contact force model is considered. This model is expressed as:

$$F_N = k\delta^{1.5}\left(1+\frac{3\left(1-e_r^{~2}\right)}{4}\frac{\dot{\delta}}{\dot{\delta}^{(-)}}\right) = k\delta^{1.5} + X\delta^{1.5}\dot{\delta} \qquad X = \frac{3\left(1-e_r^{~2}\right)}{4\dot{\delta}^{(-)}}k \qquad (4)$$

$$k = \frac{4}{3\left(h_i + h_j\right)}\left(\frac{R_i R_j}{R_i - R_j}\right)^{\frac{1}{2}} , \qquad h_k = \frac{1-\upsilon_k^{~2}}{E_k} \qquad k = i,j \qquad (5)$$

where k is the generalized stiffness constant, δ is the amount of relative penetration, e_r is the coefficient of restitution, $\dot{\delta}$ is the penetration velocity, $\dot{\delta}^{(-)}$ is the initial penetration velocity, x is the hysteresis factor, R_i and R_j are the radii of the slider hole and the guide rod, υ is the Poisson's ratio and E is the elastic modulus of the colliding bodies. It should be mentioned that the contact force model proposed by Lankarani and Nikravesh is valid when the dissipated energy during contact, as compared with the maximum absorbed elastic energy, is relatively small. Moreover, Eq. (4) is valid for impact velocities smaller than the propagation velocity of elastic waves across the two bodies; $\dot{\delta}^{(-)} \leq 10^{-5}\sqrt{E/\rho}$ where E is the Young's modulus and ρ is the material mass density. The quantity $\sqrt{E/\rho}$ is the larger of two propagation velocities of the elastic deformation waves in the impacting bodies [24]. The result of this model is compared with the Hunt and Crossley contact model described as:

$$F_N = k\delta^{1.5}\left(1+\frac{3\left(1-e_r\right)}{2}\frac{\dot{\delta}}{\dot{\delta}^{(-)}}\right) = k\delta^{1.5} + X\delta^{1.5}\dot{\delta} \qquad X = \frac{3\left(1-e_r\right)}{2\dot{\delta}^{(-)}}k \qquad (6)$$

2.3. Contact force Taylor expansion

Considering the oscillations about equilibrium position one can write,

$$y = \bar{y} + y^* \qquad (7)$$

where $\bar{y}$ is the equilibrium position of the slider and y^* is the amount of deviation from the equilibrium position. Substituting Eq. (7) into Eq. (4) and using the Taylor expansion, the contact force is written as:

$$F_N = \begin{cases} 0 & \delta \leq 0 \\ k\delta^{1.5} + X\delta^{1.5}\dot{\delta} & \delta > 0 \end{cases}$$

$$k\delta^{1.5} + X\delta^{1.5}\dot{\delta} = k\left(-y-c\right)^{1.5} + X\left(-y-c\right)^{1.5}\left(-\dot{y}\right) = k\left(-\left(\bar{y}+y^*\right)-c\right)^{1.5} + X\left(-\left(\bar{y}+y^*\right)-c\right)^{1.5}\left(-\dot{y}\right)$$

$$(8)$$

$$= k\left(\Delta - y^*\right)^{1.5} + X\left(\Delta - y^*\right)^{1.5}\left(-\dot{y}^*\right) = k\Delta^{1.5}(1 - \frac{y^*}{\Delta})^{1.5} + X\Delta^{1.5}(1 - \frac{y^*}{\Delta})^{1.5}(-\dot{y}^*)$$

$$= k\Delta^{1.5}\left(1 - \frac{3}{2}\frac{y^*}{\Delta} + \frac{3}{8}\left(\frac{y^*}{\Delta}\right)^2 + ...\right) + X\Delta^{1.5}\left(1 - \frac{3}{2}\frac{y^*}{\Delta} + \frac{3}{8}\left(\frac{y^*}{\Delta}\right)^2 + ...\right)(-\dot{y}^*)$$

$$\delta = -y - c \qquad \dot{\delta} = -\dot{y} \qquad \Delta = -\overline{y} - c$$

Substituting the resulting contact force into the equations of motion one can obtain:

$$\ddot{u} + \omega_1^2 u + \alpha_1 u^2 + \alpha_2 \dot{u} + \alpha_3 u\dot{u} + \alpha_4 u^2 \dot{u} = \alpha_5\left(\theta - \frac{\theta^3}{6}\right)\ddot{\theta} + \alpha_5 \dot{\theta}^2\left(1 - \frac{\theta^2}{2}\right) \qquad u = -y^* \tag{9}$$

$$\ddot{\theta} + \omega_2^2 \theta = \alpha_6\left(\theta - \frac{\theta^3}{6}\right)\ddot{u} + \alpha_7 \theta^3 \tag{10}$$

with

$$\omega_1^2 = \frac{3}{2}\frac{k}{m+m_1}\Delta^{0.5} \qquad \omega_2^2 = \frac{3g}{2L} \qquad \alpha_1 = \frac{3}{8}\frac{k}{m+m_1}\Delta^{-0.5} \qquad \alpha_2 = \frac{X}{m+m_1}\Delta^{1.5}$$

$$\alpha_3 = \frac{3}{2}\frac{X}{m+m_1}\Delta^{0.5} \qquad \alpha_4 = \frac{3}{8}\frac{X}{m+m_1}\Delta^{-0.5} \qquad \alpha_5 = \frac{mL}{2(m+m_1)} \qquad \alpha_6 = \frac{3}{2L} \qquad \alpha_7 = \frac{\omega_2^2}{6} \tag{11}$$

where ω_1 and ω_2 are the linear natural frequencies.

2.4. Non-contact mode

In the non-contact mode, the equations of motion are obtained by setting the contact force to be zero. These equations are expressed as,

$$\left(m+m_1\right)\ddot{y} + m\frac{L}{2}\sin(\theta)\ddot{\theta} = -\left(m+m_1\right)g - m\frac{L}{2}\dot{\theta}^2\cos(\theta) \tag{12}$$

$$m\frac{L}{2}\sin(\theta)\ddot{y} + m\frac{L^2}{3}\ddot{\theta} = -mg\frac{L}{2}\sin(\theta) \tag{13}$$

2.5. Lubrication model

The joints are designed to operate with some lubricant in most machines and mechanisms. The journal and the bearing could be kept separate from each other by high pressures produced in the lubricant. In addition, the lubricant forms a thin film which decreases friction and wear, supplies load capacity and adds damping to dissipate unwanted mechanical vibrations. When a fluid is squeezed between two approaching surfaces, the squeeze forces are generated. In journal bearings, when the relative rotational velocity is small with respect to the relative radial velocity, the squeeze action is governing and hence, it is rational to neglect the wedge term in the Reynolds' equation. Integrating the pressure field over the surface of the journal, the resulting force *F* on the journal that equilibrates the fluid pressure is calculated as in [25]:

$$F = \frac{12\pi\mu L_{JB} R_J^3}{c^2 \left(1-\varepsilon^2\right)^{3/2}} \dot{\varepsilon} \qquad\qquad \varepsilon = \frac{-y}{c} \tag{14}$$

where μ is the dynamic lubricant viscosity, L_{JB} is the journal bearing length, R_J is the journal radius, c is the radial clearance, ε is the eccentricity ratio and $\dot{\varepsilon}$ is the time rate of change for the eccentricity ratio. Eq. (14) is derived for infinitely long journal bearing in which the length-to-diameter ratio is larger than 2. Since the squeeze force is proportional to the rate of decrease of the fluid film thickness, it is obvious that the lubricant resists the load as a nonlinear viscous damper when the film thickness is reducing [25]. However, the fluid could have the spring role as well. In this paper, it is assumed that the fluid acts as a linear spring and a nonlinear viscous damper. Therefore, the behavior of the fluid is described as,

$$F = \frac{12\pi\mu L_{JB} R_J^3}{c^2 \left(1-\varepsilon^2\right)^{3/2}} \dot{\varepsilon} + k\left(-y\right) = D\frac{\dot{\varepsilon}}{\left(1-\varepsilon^2\right)^{3/2}} - ky \qquad D = \frac{12\pi\mu L_{JB} R_J^3}{c^2} \tag{15}$$

This force is substituted into Eq. (1) instead of the contact force to achieve new equations of motion. These new equations are valid when the lubricated journal and the bearing are not in contact. This force could be expanded using Eq. (7) as,

$$F = D\frac{\dot{\varepsilon}}{\left(1-\varepsilon^2\right)^{3/2}} - ky = D\left(\frac{-\dot{y}}{c}\right)\left(1-(\frac{\overline{y}+y^*}{c})^2\right)^{-3/2} - k(\overline{y}+y^*)$$

$$= D\left(\frac{\dot{u}}{c}\right)(1+\frac{3}{2}(\frac{\overline{y}+y^*}{c})^2) - k(\overline{y}+y^*) = D\left(\frac{\dot{u}}{c}\right)(1+\frac{3}{2c^2}(u^2 - 2\overline{y}u + \overline{y}^2)) + ku - k\overline{y} \qquad u = -y^* \tag{16}$$

Substituting the expanded force into the equations of motion one obtains,

$$\ddot{u} + \hat{\omega}_1^2 u + \hat{\alpha}_1\dot{u} + \hat{\alpha}_2 u\dot{u} + \hat{\alpha}_3 u^2\dot{u} = \hat{\alpha}_4\left(\theta - \frac{\theta^3}{6}\right)\ddot{\theta} + \hat{\alpha}_4\dot{\theta}^2\left(1-\frac{\theta^2}{2}\right) \tag{17}$$

$$\ddot{\theta} + \omega_2^2\theta = \hat{\alpha}_5\left(\theta - \frac{\theta^3}{6}\right)\ddot{u} + \hat{\alpha}_6\theta^3 \tag{18}$$

with

$$\hat{\omega}_1^2 = \frac{k}{m+m_1} \qquad \omega_2^2 = \frac{3g}{2L} \qquad \hat{\alpha}_1 = \frac{D}{(m+m_1)c}(1+\frac{3\overline{y}^2}{2c^2}) \qquad \hat{\alpha}_2 = \frac{-3D\overline{y}}{(m+m_1)c^3}$$

$$\hat{\alpha}_3 = \frac{3D}{2(m+m_1)c^3} \qquad \hat{\alpha}_4 = \frac{mL}{2(m+m_1)} \qquad \hat{\alpha}_5 = \frac{3}{2L} \qquad \hat{\alpha}_6 = \frac{\omega_2^2}{6} \tag{19}$$

3. Nonlinear vibration analysis using the method of multiple scales

In mathematics and physics, the method of multiple scales consists of the techniques used to make uniformly valid approximations to the solutions of perturbation problems both for small as well as large values of the independent variables. This is carried out by introducing fast-scale and slow-scale variables for an independent variable and then treating these variables, fast and slow,

as though they are independent. The consequent extra freedom presented by the new independent variables is employed to eliminate unwanted secular terms in the solution process of the perturbation problem. The latter puts restraints on the approximate solution which are called solvability conditions [26]. The fundamental notion of the method of multiple scales is to consider the expansion denoting the response to be a function of multiple independent variables, or scales, in place of a single variable. This method can deal with damped systems conveniently [27]. Although with this method one can qualitatively understand the effect of different parameters in the vibrational response of a nonlinear system and have an insight into the frequency response of the system, it has some restrictions as well. Handling the weak nonlinearities and its limitation in solving some nonlinear problems could be a defect for the versatility of this method. To show the application of this method for a system with clearance, it is used to solve Eqs. (9-10) and Eqs. (17-18) in the subsequent section.

3.1. Analytical solution

In order to implement the method of multiple scales to solve the equations analytically, one assumes that the solution can be represented by an expansion in the following form:

$$u = u_0(T_0, T_1) + \varepsilon u_1(T_0, T_1), \quad \theta = \theta_0(T_0, T_1) + \varepsilon \theta_1(T_0, T_1), \quad T_0 = t, \ T_1 = \varepsilon t \tag{20}$$

where T_0 and T_1 are independent time scales. The derivatives with respect to t turn into expansions in terms of the partial derivatives with respect to T_0 and T_1 according to,

$$\frac{d}{dt} = \frac{dT_0}{dt}\frac{\partial}{\partial T_0} + \frac{dT_1}{dt}\frac{\partial}{\partial T_1} + \ldots = D_0 + \varepsilon D_1 + \ldots$$

$$\frac{d^2}{dt^2} = D_0^2 + 2\varepsilon D_0 D_1 + \varepsilon^2\left(D_1^2 + 2D_0 D_1\right) + \ldots \tag{21}$$

3.1.1. Dry contact

The damping and nonlinearities tend to counter the influence of the resonances [28]. If they exist, they are scaled by ε to appear in the second equation (ε is a small dimensionless parameter and not the eccentricity ratio). Equating the identical powers of ε^0 yields,

$$D_0^2 u_0 + \omega_1^2 u_0 = 0 \quad \rightarrow \quad u_0 = A(T_1) e^{i\omega_1 T_0} + \bar{A}(T_1) e^{-i\omega_1 T_0} \tag{22}$$

$$D_0^2 \theta_0 + \omega_2^2 \theta_0 = 0 \quad \rightarrow \quad \theta_0 = B(T_1) e^{i\omega_2 T_0} + \bar{B}(T_1) e^{-i\omega_2 T_0} \tag{23}$$

Then equating the identical powers of ε^1 yields,

$$D_0^2 u_1 + \omega_1^2 u_1 = -0.5\alpha_5\left(D_0\theta_0\right)^2\theta_0^2 + \alpha_5\left(D_0^2\theta_0\right)\theta_0 - 2D_0 D_1 u_0 - \left(D_0 u_0\right)\alpha_3 u_0 - \left(D_0 u_0\right)\alpha_4 u_0^2$$

$$-\alpha_2 D_0 u_0 - \alpha_1 u_0^2 + \alpha_5\left(D_0\theta_0\right)^2 - \frac{1}{6}\alpha_5\left(D_0^2\theta_0\right)\theta_0^3 \tag{24}$$

$$D_0^2\theta_1 + \omega_2^2\theta_1 = -2D_0 D_1\theta_0 + \alpha_7\theta_0^3 + \alpha_6\left(D_0^2 u_0\right)\theta_0 - \frac{1}{6}\alpha_6\left(D_0^2 u_0\right)\theta_0^3 \tag{25}$$

Substituting the solutions of Eqs. (22-23) into Eqs. (24-25), the secular terms are derived as,

$$-IA\,\alpha_2\omega_1 - IA^2\bar{A}\,\alpha_4\omega_1 - 2I\,\omega_1 D_1 A = 0 \tag{26}$$

$$3\alpha_7 B^2\bar{B} - 2I\,\omega_2 D_1 B = 0 \tag{27}$$

It is convenient to express $A(T_1)$ and $B(T_1)$ in polar forms as,

$$A(T_1) = \frac{1}{2}a(T_1)e^{I\beta(T_1)} \tag{28}$$

$$B(T_1) = \frac{1}{2}b(T_1)e^{I\gamma(T_1)} \tag{29}$$

Substituting into secular terms one obtains,

$$\omega_1 a\dot{\beta} = 0 \quad\rightarrow\quad \beta = c_2 \tag{30}$$

$$-\frac{1}{2}a\alpha_2\omega_1 - \frac{1}{8}a^3\alpha_4\omega_1 - \omega_1\dot{a} = 0 \rightarrow a = \frac{2\sqrt{\alpha_2}}{\sqrt{4\alpha_2 c_1 e^{\alpha_2 t_1} - \alpha_4}} \tag{31}$$

$$i\omega_2\dot{b} = 0 \rightarrow b = c_3 \tag{32}$$

$$\omega_2\dot{\gamma} + \frac{3}{8}\alpha_7 b^2 = 0 \rightarrow \gamma = -\frac{3}{8}\frac{c_3^2\alpha_7 T_1}{\omega_2} + c_4 \tag{33}$$

where c_1, c_2, c_3, c_4 are constants and are determined by initial conditions. The dynamic response can be written as,

$$\theta = c_3\cos\left(\frac{-3T_1\alpha_7 c_3^2 + 8T_0\omega_2^2 + 8\omega_2 c_4}{8\omega_2}\right) \tag{34}$$

$$
\begin{aligned}
y = &-0.0833\frac{\alpha_5\omega_2^2 c_3^4\omega_1^2\cos\left(\frac{-3T_1\alpha_7 c_3^2 + 8T_0\omega_2^2 + 8c_4\omega_2}{2\omega_2}\right)}{\omega_1^4 - 20\omega_1^2\omega_2^2 + 64\omega_2^4} + \\
&0.3333\frac{\alpha_5\omega_2^4 c_3^4\cos\left(\frac{-3T_1\alpha_7 c_3^2 + 8T_0\omega_2^2 + 8c_4\omega_2}{2\omega_2}\right)}{\omega_1^4 - 20\omega_1^2\omega_2^2 + 64\omega_2^4} - \frac{1}{12}\frac{\alpha_5\omega_2^2 c_3^4\cos\left(\frac{-3T_1\alpha_7 c_3^2 + 8T_0\omega_2^2 + 8c_4\omega_2}{4\omega_2}\right)}{\omega_1^2 - 4\omega_2^2} + \\
&\frac{\alpha_5\omega_2^2 c_3^2\omega_1^2\cos\left(\frac{-3T_1\alpha_7 c_3^2 + 8T_0\omega_2^2 + 8c_4\omega_2}{4\omega_2}\right)}{\omega_1^4 - 20\omega_1^2\omega_2^2 + 64\omega_2^4} - \frac{16\alpha_5\omega_2^4 c_3^2\cos\left(\frac{-3T_1\alpha_7 c_3^2 + 8T_0\omega_2^2 + 8c_4\omega_2}{4\omega_2}\right)}{\omega_1^4 - 20\omega_1^2\omega_2^2 + 64\omega_2^4} - \\
&\frac{2}{3}\frac{\alpha_2\alpha_1\cos(2\omega_1 T_0 + 2c_2)}{\omega_1^2\left(4\alpha_2 c_1 e^{\alpha_2 T_1} - \alpha_4\right)} + \frac{2}{3}\frac{\alpha_2\alpha_3\sin(2\omega_1 T_0 + 2c_2)}{\omega_1\left(4\alpha_2 c_1 e^{\alpha_2 T_1} - \alpha_4\right)} + \\
&+\frac{1}{4}\frac{\alpha_2\left(\sqrt{\alpha_2}\,\alpha_4\omega_1\sin(3\omega_1 T_0 + 3c_2) + 8\alpha_1\sqrt{4\alpha_2 c_1 e^{\alpha_2 T_1} - \alpha_4}\right)}{\left(4\alpha_2 c_1 e^{\alpha_2 T_1} - \alpha_4\right)^{3/2}\omega_1^2} - \frac{2\sqrt{\alpha_2}\cos(\omega_1 T_0 + c_2)}{\sqrt{4\alpha_2 c_1 e^{\alpha_2 T_1} - \alpha_4}} - 5.0590\times10^{-4}
\end{aligned}
\tag{35}
$$

The last four terms of the *y* solution decays exponentially with time and vanishes when the system reaches its steady state. The first five terms represent the steady state response. After the system reaches its steady state, the slider oscillates with two frequencies described as,

$$\frac{-12\alpha_7 c_3^2 + 32\omega_2^2}{8\omega_2} = \frac{-12(\frac{\omega_2^2}{6})c_3^2 + 32\omega_2^2}{8\omega_2} = 4\omega_2 - \frac{1}{4}c_3^2\omega_2 = 2.44Hz \tag{36}$$

$$\frac{-6\alpha_7 c_3^2 + 16\omega_2^2}{8\omega_2} = \frac{-6(\frac{\omega_2^2}{6})c_3^2 + 16\omega_2^2}{8\omega_2} = 2\omega_2 - \frac{1}{8}c_3^2\omega_2 = 1.219Hz \tag{37}$$

In addition, the pendulum oscillates with the following frequency,

$$\frac{-3\alpha_7 c_3^2 + 8\omega_2^2}{8\omega_2} = \frac{-3(\frac{\omega_2^2}{6})c_3^2 + 8\omega_2^2}{8\omega_2} = \omega_2 - \frac{1}{16}c_3^2\omega_2 = 0.6094Hz \tag{38}$$

As can be seen, when transient response vanishes, the slider oscillates with frequencies which are dependent on the linear natural frequency corresponding to the pendulum oscillation (ω_2) and the square of the amplitude of the pendulum. This means that in the steady state, the first linear natural frequency (ω_1) which is associated to the vertical displacement of the slider is not involved in the response. Furthermore, the pendulum angle is not affected by the vertical displacement of the slider as can be seen from Eq. (34). Therefore, it could be deduced that the pendulum motion affects the steady state vertical displacement of the slider but the opposite effect could be negligible.

3.1.2. Non-contact mode solution

When the slider and the guide are not in contact, Eqs. (12-13) have to be solved. The solution for the pendulum angle is achieved as,

$$\theta = c_3 \cos(bt - c_4) \qquad b = \left(-0.0625\varepsilon c_3^2 + 0.0625\varepsilon c_3^2 + 0.5\varepsilon - 1\right)\omega_2 \qquad \omega_2^2 = \frac{3g}{2L} \tag{39}$$

Substituting Eq. (39) into Eq. (12) and integrating twice, the vertical position of the slider is calculated as,

$$
\begin{aligned}
y = & -0.3333\beta_1 c_3^4 \sin(c_4)\cos^3(c_4)\sin(bt)\cos^3(bt) + 0.1667\beta_1 c_3^4 \sin(c_4)\cos(c_4)\sin(bt)\cos^3(bt) \\
& +0.1667\beta_1 c_3^4 \sin(c_4)\cos^3(c_4)\sin(bt)\cos(bt) - 0.1667\beta_1 c_3^4 \sin(c_4)\cos(c_4)\sin(bt)\cos(bt) \\
& +\beta_1 c_3^2 \sin(c_4)\cos(c_4)\sin(bt)\cos(bt) - 0.0417\beta_1 c_3^4 \cos^4(bt) + 0.0833\beta_1 c_3^4 \cos^2(bt) \\
& -0.5\beta_1 c_3^2 \cos^2(bt) - 0.3333\beta_1 c_3^4 \cos^4(c_4)\cos^4(bt) + 0.3333\beta_1 c_3^4 \cos^2(c_4)\cos^4(bt) \\
& +0.3333\beta_1 c_3^4 \cos^4(c_4)\cos^2(bt) - 0.0417\beta_1 c_3^4 \cos^2(c_4)\cos^2(bt) + \beta_1 c_3^2 \cos^2(c_4)\cos^2(bt) \\
& -0.5gt^2 + 6.25\times10^{-12}\beta_1 c_3^4 b^2 t^2 - 1.25\times10^{-11}\beta_1 c_3^4 bc_4 t + \beta_1 c_3^2 bc_4 t - 0.0417\beta_1 c_3^4 \cos^4(c_4) \\
& +0.0833\beta_1 c_3^4 \cos^2(c_4) - 0.5\beta_1 c_3^2 \cos^2(c_4) - 0.02604\beta_1 c_3^4 + 0.25\beta_1 c_3^2 + c_1 t + c_2 \\
\beta_1 = & -\frac{mL}{2(m + m_1)}
\end{aligned}
\tag{40}
$$

The term $-1/2\,gt^2$ of the solution is related to the free fall of the system (including the guide and the slider) because no external force is applied to the system except its weight. Furthermore, the trigonometric parts of the solution could be due to the rotational motion of the pendulum relative to the guide when the system falls freely. For contact and non-contact phases, their corresponding solutions are used to determine the system response. In each transition from the non-contact phase to the contact phase or vice versa, the initial conditions for the new phase are the same as the conditions at the end of the previous one and should be used to determine the solution constants.

3.1.3. Lubricated joint

Following the procedure in section 3.1.1, the steady solution of Eqs. (17-18) are obtained as,

$$\theta = c_3 \cos\left(\frac{-3T_1\hat{\alpha}_6 c_3^2 + 8T_0\omega_2^2 + 8\omega_2 c_4}{8\omega_2}\right)$$

(41)

$$
y = -0.0833 \frac{\hat{\alpha}_4 \omega_2^2 c_3^4 \hat{\omega}_1^2 \cos\left(\frac{-3T_1\hat{\alpha}_6 c_3^2 + 8T_0\omega_2^2 + 8c_4\omega_2}{2\omega_2}\right)}{\hat{\omega}_1^4 - 20\hat{\omega}_1^2\omega_2^2 + 64\omega_2^4} + 0.3333 \frac{\hat{\alpha}_4 \omega_2^4 c_3^4 \cos\left(\frac{-3T_1\hat{\alpha}_6 c_3^2 + 8T_0\omega_2^2 + 8c_4\omega_2}{2\omega_2}\right)}{\hat{\omega}_1^4 - 20\hat{\omega}_1^2\omega_2^2 + 64\omega_2^4} -
$$
$$
\frac{1}{12} \frac{\hat{\alpha}_4 \omega_2^2 c_3^4 \hat{\omega}_1^2 \cos\left(\frac{-3T_1\hat{\alpha}_6 c_3^2 + 8T_0\omega_2^2 + 8c_4\omega_2}{4\omega_2}\right)}{\hat{\omega}_1^4 - 20\hat{\omega}_1^2\omega_2^2 + 64\omega_2^4} + \frac{4}{3} \frac{\hat{\alpha}_4 \omega_2^4 c_3^4 \cos\left(\frac{-3T_1\hat{\alpha}_6 c_3^2 + 8T_0\omega_2^2 + 8c_4\omega_2}{4\omega_2}\right)}{\hat{\omega}_1^4 - 20\hat{\omega}_1^2\omega_2^2 + 64\omega_2^4} -
$$
$$
\frac{16\hat{\alpha}_4 \omega_2^4 c_3^2 \cos\left(\frac{-3T_1\hat{\alpha}_6 c_3^2 + 8T_0\omega_2^2 + 8c_4\omega_2}{4\omega_2}\right)}{\hat{\omega}_1^4 - 20\hat{\omega}_1^2\omega_2^2 + 64\omega_2^4} + \frac{\hat{\omega}_1^2 \hat{\alpha}_4 \omega_2^2 c_3^2 \cos\left(\frac{-3T_1\hat{\alpha}_6 c_3^2 + 8T_0\omega_2^2 + 8c_4\omega_2}{4\omega_2}\right)}{\hat{\omega}_1^4 - 20\hat{\omega}_1^2\omega_2^2 + 64\omega_2^4} - 3.1568 \times 10^{-7}
$$

(42)

Similar to dry contact, in the steady state, the first linear natural frequency corresponding to the vertical displacement of the slider ($\hat{\omega}_1$) is not involved in the response and the slider oscillates with frequencies which are dependent on the linear natural frequency corresponding to the pendulum oscillation (ω_2) and the square of the amplitude of the pendulum.

3.2. Primary resonance

If a high frequency harmonic external force is applied on the slider vertically, a primary resonance could happen. This high frequency external force could be generated if a high-speed motor mounted on the slider has an unbalance mass. The external force term $F = F_0 \cos(\Omega t)$ is scaled by ε to appear in the second equation for primary resonance. To show quantitatively the nearness of the primary resonance, the detuning parameter σ is introduced defined as follows,

$$\Omega = \omega_1 + \varepsilon\sigma$$

(43)

Substituting Eq. (43) into the equations of motion and using the method of multiple scales, the secular term will change as,

$$-2i\,\omega_1 D_1 A - i\,\alpha_4 A^2 \bar{A}\,\omega_1 - i\,\alpha_2 A\,\omega_1 + \frac{1}{2}F_0 e^{i\sigma T_1} = 0$$

(44)

Using Eq. (28) and separating imaginary and real parts one can write,

$$\omega_1 a \beta' + \frac{1}{2} F_0 \cos(\Phi) = 0 \quad , \quad -\omega_1 a' - \frac{1}{8} \alpha_4 a^3 \omega_1 - \frac{1}{2} \alpha_2 a \omega_1 + \frac{1}{2} F_0 \sin(\Phi) = 0 \quad , \quad \Phi = \sigma T_1 - \beta \quad (45)$$

where the prime denotes the derivative with respect to T_1. The steady state response corresponds to $a' = \Phi' = 0$. After squaring and adding the equations, the frequency response is achieved as,

$$\sigma^2 + \left(\frac{1}{8} \alpha_4 a^2 + \frac{1}{2} \alpha_2 \right)^2 = \frac{F_0^2}{4 \omega_1^2 a^2} \quad (46)$$

Following the same procedure the frequency response for the lubricated clearance joint is obtained:

$$\sigma^2 + \left(\frac{1}{8} \hat{\alpha}_3 a^2 + \frac{1}{2} \hat{\alpha}_1 \right)^2 = \frac{F_0^2}{4 \hat{\omega}_1^2 a^2} \quad (47)$$

4. Results and discussion

The properties of the system used in the simulation are listed in Table 1. The initial angular position of the pendulum is 10 degrees and it is initially at rest. The initial vertical position and velocity of the slider are -0.000499 m and 0 m/s respectively. The slider is thus not in contact with the guide initially. Firstly, the equations of motion are integrated numerically using the Runge-Kutta-Fehlberg method [29]. These equations are then solved analytically when the slider and guide are in contact to see the effect of surface elasticity on the dynamic and vibrational response of the system. The impact velocity could be calculated from the non-contact solution and substituted into the contact force model instead of $\dot{\delta}^{(-)}$ to determine the hysteresis factor X.

Table 1. The properties of the sliding pendulum used in simulation

Parameters	Values	Units
Pendulum mass	50	kg
Slider mass	0.2	kg
Pendulum length	1	m
Modulus of elasticity	200	GPa
Poisson's ratio	0.3	-
Radius of slider hole	0.0055	m
Radius of rod	0.005	m
Clearance	0.5	mm

4.1. Effect of contact force terms in Taylor expansion

The results of numerical solution (vertical position of the slider) for the equations of motion in three cases are shown in Fig. 2. The first case relates to the contact force described by Eq. (4) and the other two cases are related to the equations of motion in which the contact force is replaced by the Taylor expansion with the first two and three terms presented in Eq. (8). Both contact and non-contact phases are considered in the solution code. Therefore, when the amount of penetration is positive, the contact force is included in the equations of motion. Otherwise, it is set to be zero. As can be seen, a relatively good agreement exists between the results. It is thus

concluded that replacing the contact force by the first two or three Taylor expansion terms can make a negligible error. This substitution is accomplished to apply the analytical method.

4.2. Verification

Results from numerical and analytical solutions are shown in Fig. 3. One contact happens as pointed out in the figure. The two terms of the Taylor expansion are used for the dissipation part of the contact force model ($\alpha_4 = 0$). As it can be seen, the results are in an acceptable agreement with each other. The exact result for the pendulum angle is obtained with just the first expansion term while the vertical position of the slider is plotted using two terms in permanent contact mode. The non-contact response is plotted with black dashed line in Fig. 3a obtained from the analytical solution of Section 3.1.2 for the non-contact mode.
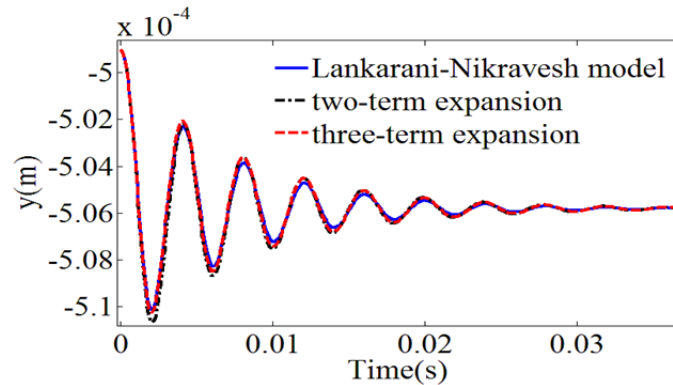

Fig. 2. Vertical position of the slider with and without Taylor expansion obtained from numerical simulation

The multiple scales method could obtain a closed-form solution to the problem which provides a deeper insight into the dynamic and vibrational behavior of the system. The effect of the surface elasticity (contact) on the dynamic response can be pursued in the closed-form solution. In addition, some vibrational analysis such as investigating primary resonance in the presence of external force is available when using the multiple scales method.
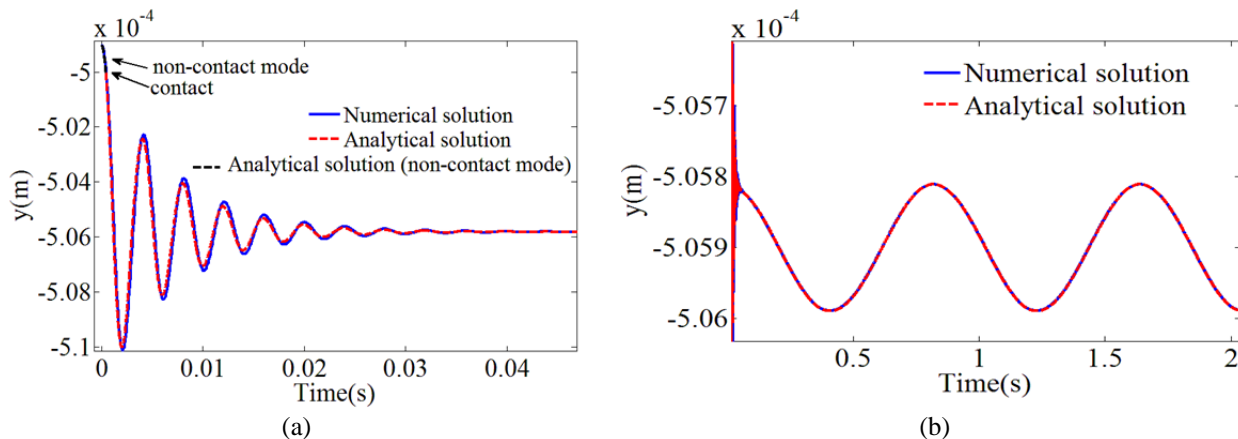

(a)

(b)

Fig. 3. Comparison of the numerical and analytical (multiple scales method) responses, (a) slider vertical position, (b) steady state slider vertical position, (c) pendulum angle
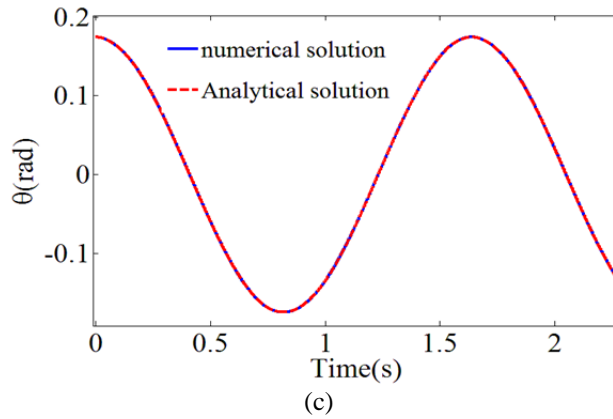
(c)

Fig. 3. (Cont.)

4.3. Primary resonance for dry contact

The frequency response for different clearance sizes are plotted in Fig. 4. The rod's radius is set to be 0.005 m as before but the radius of the slider's hole varies to change the clearance size. The amplitude of the external force is chosen to be 10 N. According to Eq. (5), changing the radius of the hole changes the generalized stiffness correspondingly. The stiffness affects the coefficients α_2, α_4 and ω_1 as can be perceived from Eq. (11) and this issue changes the frequency response (see Eq. (46)). The frequency response then changes when the radius of the hole and the resulting clearance size varies. As seen, the amplitude of the vertical position of the slider increases in the vicinity of the first linear natural frequency. If the energy dissipation term is not taken into account in the contact force model, this amplitude may increase so much that the system could get exposed to failure. By considering this material damping term, the amplitude is bounded as shown in Fig. 4. Decreasing the outer radius and the resulting clearance size decreases the amplitude in the vicinity of the linear natural frequency as can be apparently seen. In addition, decreasing the coefficient of restitution makes the frequency response come down. This was expected due to increasing the material damping when the coefficient of restitution decreases.
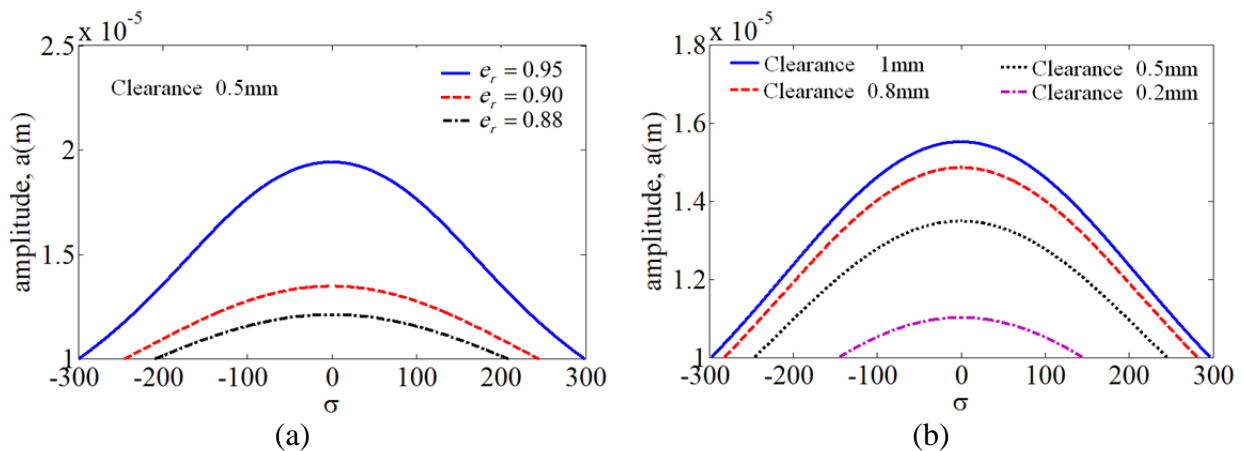

(a)   (b)

Fig. 4. Frequency response (a) for different coefficients of restitution, (b) for different clearance sizes

4.4. Frequency analysis

In this section, analysis of the system response is carried out in frequency domain. For this purpose, the Fast Fourier Transform is used and FFT plots for vertical displacement of the slider w.r.t the steady state equilibrium position and pendulum angle are shown in Fig. 5(a-c). Fast Fourier Transform is performed on the numerical results to compare the frequencies of the response with those of the closed-form solution obtained from analytical method. As expected, the obtained frequencies match well with the results in section 3.1.1 in Eqs. (37-38). The frequency 252.7 Hz corresponds to the frequency ω_1 in the transient response. Frequencies in the closed-form solution like $2\omega_1$ and 2.44 Hz are not achieved in FFT analysis because the amplitudes of the terms containing these frequencies are small compared to others. It is therefore concluded that implementing an analytical method could give a deeper insight into the dynamic response of mechanical systems which is not fully obtained when treating the problem numerically.
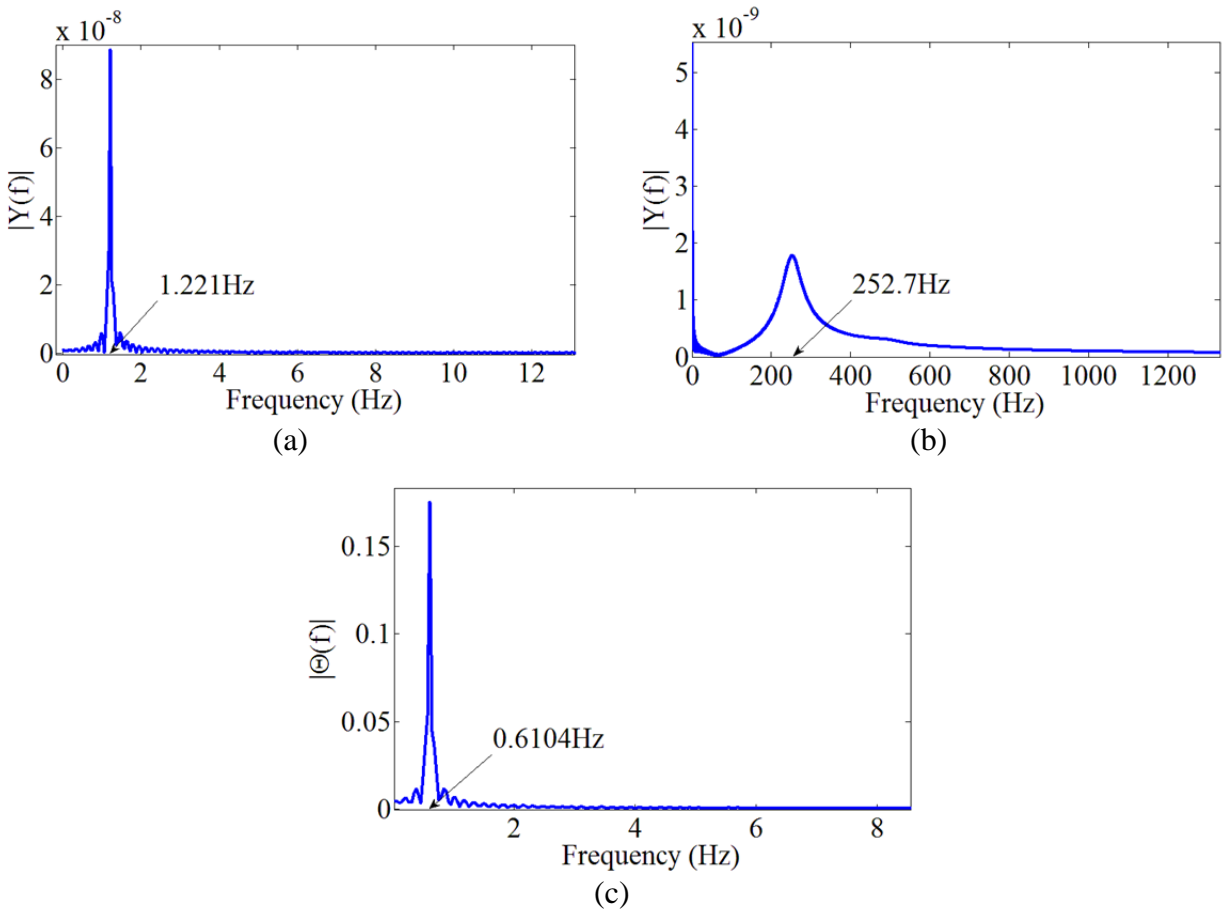
Fig. 5. FFT plots, (a, b) for vertical displacement of the slider w.r.t the steady state equilibrium position, (c) pendulum angle

4.5. Hunt-Crossly contact force model

In this section, a comparison is made between the contact force models of Lankarani-Nikravesh and Hunt-Crossly. For this purpose, the vertical position and velocity of the slider and the frequency response around the primary resonance are plotted in Fig. 6(a-c) for the two models. As can be seen, the vertical position of the slider for both models are nearly the same except that the amplitudes for the Hunt-Crossly model is slightly less than the other. Comparing the frequency response shows that in the Hunt-Crossly contact force model, the amplitude is more bounded. These comparisons reveal that the Hunt-Crossly contact force model shows a slightly more dissipative behavior.


(a)

(b)

(c)
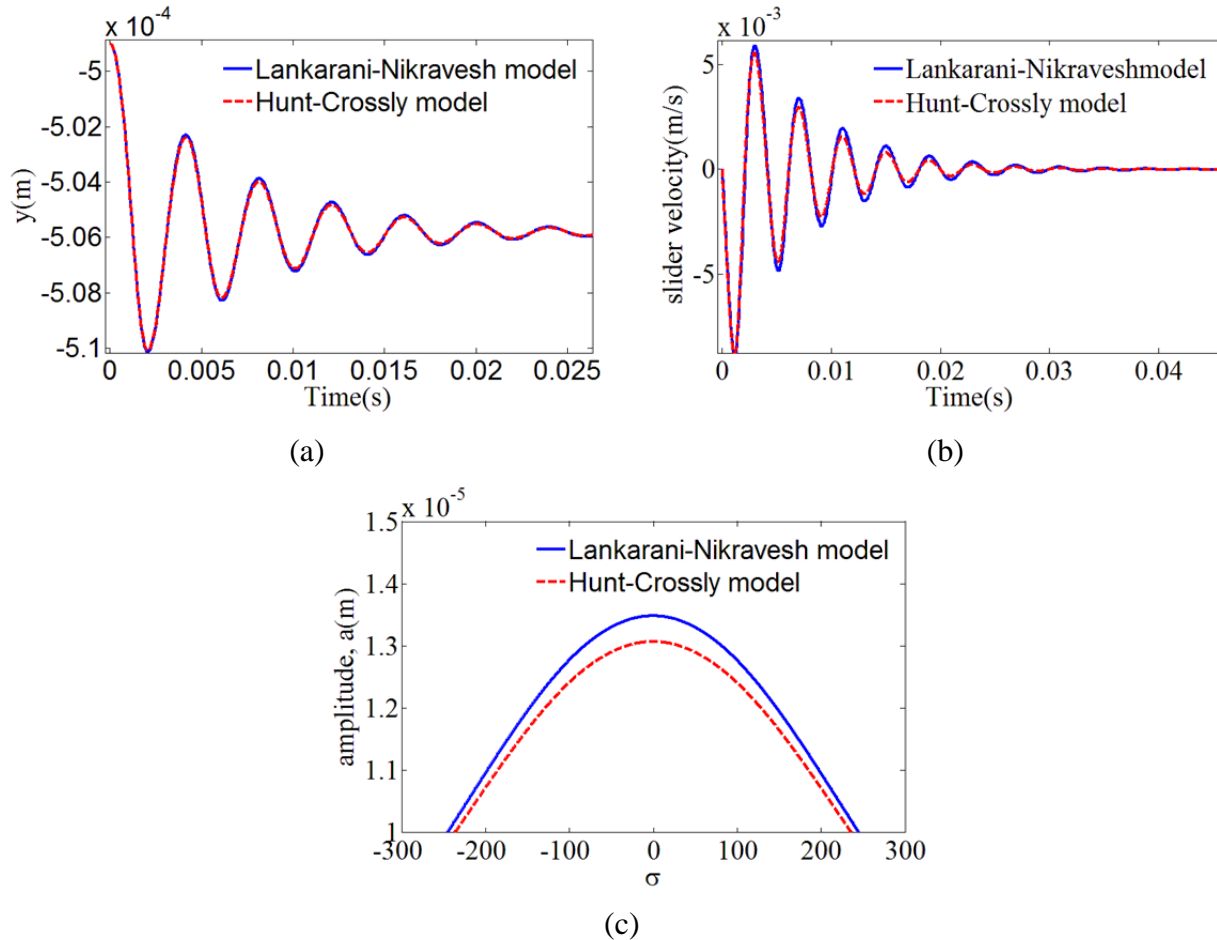
Fig. 6. Comparison between Lankarani-Nikravesh and Hunt-Crossly models: (a) vertical position of the slider, (b) vertical velocity of the slider and (c) frequency response for clearance size 0.5 mm

4.6. Lubricated joint

The vertical position of the slider obtained numerically and analytically (multiple scales method) are compared in Fig. 7. The clearance size is set to be 0.08 mm, the journal bearing length is 40 mm and the oil viscosity at 40° C is set to 400 cP. The stiffness constant corresponding to the fluid is chosen according to the range presented in [20] and is set to be $1.56 \times 10^9 \, N/m$. The initial

angular position of the pendulum is 10 degrees and it is initially at rest. The journal and the bearing centers are coincident initially and the initial slider velocity is zero. For the above properties, no solid to solid contact happens in this simulation. The results are found in an acceptable agreement with each other. The effect of the fluid characteristics on the steady state dynamic response can be investigated in the closed-form solution. As it is apparent from Eq. (42), only the fluid stiffness has influence on the amplitude of the steady state response (see $\hat{\omega}_1$) and the fluid does not make any effect on the response frequencies after the transient response vanishes.

(a)

(b)
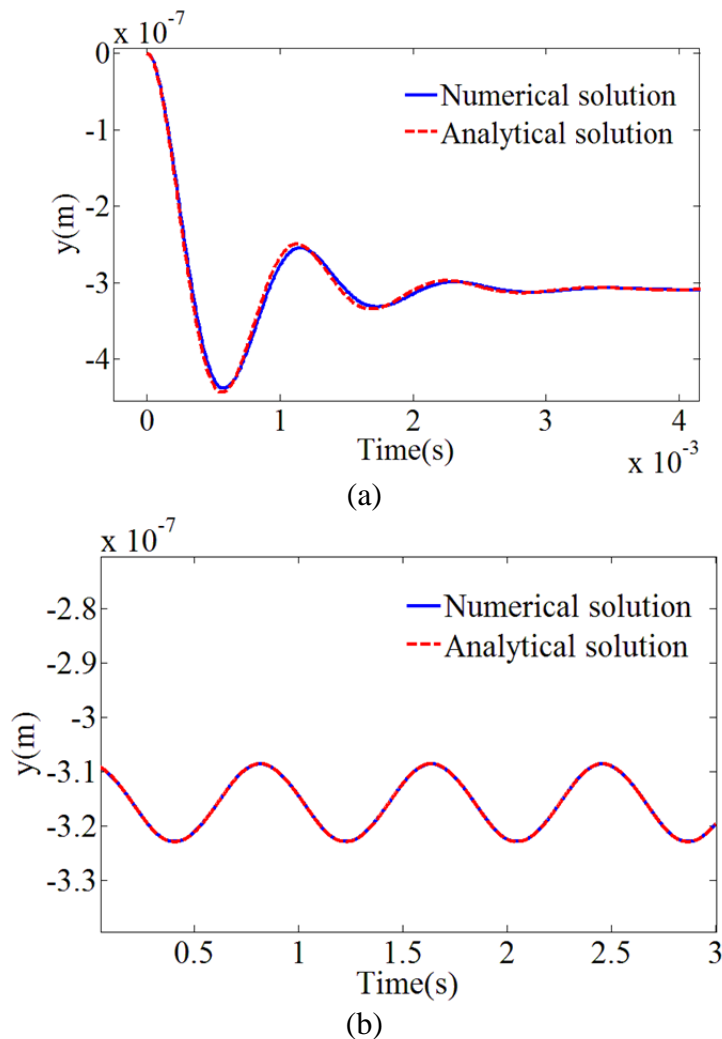
Fig. 7. Comparison of the vertical position of the slider obtained numerically and analytically for the lubricated joint case: (a) transient response, (b) steady state response

4.7. Primary resonance for the lubricated joint

The frequency response for different dynamic lubricant viscosities are plotted in Fig. 8. The amplitude of the external force is chosen to be 10 N. Equation (47) is used to plot the frequency response. Changing the dynamic lubricant viscosity changes the terms $\hat{\alpha}_1$ and $\hat{\alpha}_3$ in the

frequency response equation. As expected, increasing the dynamic lubricant viscosity decreases the amplitude in the vicinity of the linear natural frequency.
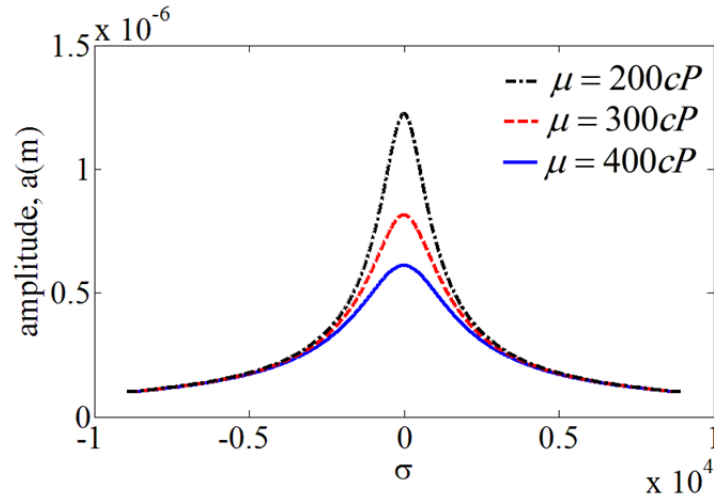

Fig. 8. Frequency response for different dynamic lubricant viscosities

It is worth to note that, according to the relations (15) and (19), changing the dynamic lubricant viscosity μ, changes $\hat{\alpha}_3$ and consequently the frequency response is changed as shown in Fig. 8. So, the nonlinear damping term $\hat{\alpha}_3 u^2 \dot{u}$ affects the amplitude of the slider in the frequency response curve. In addition, the coefficient $\hat{\alpha}_2$ in $\hat{\alpha}_2 u \dot{u}$ does not appear in the frequency response because substituting $u_0 = A(T_1) e^{i \omega T_0} + \bar{A}(T_1) e^{-i \omega T_0}$ and its first derivative in the aforementioned term does not produce any secular term. The same reasoning could be made for the frequency response for the dry contact case.

Furthermore, the cubic nonlinear stiffness term θ^3 which has the role of a soft spring in the second equation of motion, i.e. Eqs. (10) and (18), could bend the frequency response curve to the left if an external harmonic moment is applied to the pendulum.

5. Conclusion

In this study, the multiple scales method was used to perform a nonlinear vibrational analysis of a sliding pendulum in two cases with dry and lubricated clearance joint. The momentum exchange approach was used to model the clearance. In the dry contact case, the surface elasticity was modeled as a nonlinear spring and a nonlinear damper presented by the Lankarani-Nikravesh contact force model.

The dynamic response obtained analytically was in an acceptable agreement with the numerical results. Applying a harmonic excitation on the slider, the frequency response was plotted in the primary resonance condition. It was observed that decreasing the outer radius and the resulting clearance size decreases the amplitude in the vicinity of the linear natural frequency. In addition, decreasing the coefficient of restitution makes the frequency response come down. Fast Fourier Transform was performed on the numerical results to compare the frequencies of the response with those of the closed-form solution obtained from analytical method. As expected, the obtained frequencies were in good agreement with each other. The dynamic response using

Lankarani-Nikravesh contact force model was compared with Hunt-Crossly contact force model. The vertical positions of the slider for both models were nearly the same except that the amplitudes for the Hunt-Crossly model were slightly smaller. Comparing the frequency response showed that in the Hunt-Crossly contact force model, the amplitude was more bounded. Therefore, the Hunt-Crossly contact force model showed a slightly more dissipative behavior. In the lubricated joint case, a linear spring and a nonlinear damper based on the Reynolds equation developed for Sommerfeld's boundary conditions were used to model the lubricant behavior. A closed-form solution for the response of the system with lubricated joint was obtained. It was shown that only the fluid stiffness had influence on the amplitude of the steady state response and the fluid did not make any effect on the response frequencies after the transient response vanished. The steady state response frequency for both dry and lubricated clearance joints was dependent on the linear natural frequency corresponding to the pendulum oscillation. In the primary resonance analysis, increasing the dynamic lubricant viscosity decreases the amplitude in the vicinity of the linear natural frequency as expected.

References

[1] P. Flores, J. Ambrósio, Revolute joints with clearance in multibody systems, Computers & Structures, 82 (2004) 1359-1369.

[2] S. Dubowsky, F. Freudenstein, Dynamic analysis of mechanical systems with clearances, Part I: Formation of dynamic model, Journal of Engineering for Industry, (1971) 305–309.

[3] J. Rhee, A. Akay, Dynamic response of a revolute joint with clearance, Mechanism and Machine Theory, 31 (1996) 121-134.

[4] P. Ravn, A continuous analysis method for planar multibody systems with joint clearance, Multibody System Dynamics, 2 (1998) 1-24.

[5] A.L. Schwab, J.P. Meijaard, P. Meijers, A comparison of revolute joint clearance models in the dynamic analysis of rigid and elastic mechanical systems, Mechanism and Machine Theory, 37 (2002) 895-913.

[6] P. Flores, J. Ambrósio, J.P. Claro, Dynamic analysis for planar multibody mechanical systems with lubricated joints, Multibody System Dynamics, 12 (2004) 47-74.

[7] Q. Tian, Y. Zhang, L. Chen, P. Flores, Dynamics of spatial flexible multibody systems with clearance and lubricated spherical joints, Computers & Structures, 87 (2009) 913-929.

[8] Q. Tian, C. Liu, M. Machado, P. Flores, A new model for dry and lubricated cylindrical joints with clearance in spatial flexible multibody systems, Nonlinear Dynamics, 64 (2011) 25-47.

[9] V.L. Reis, G.B. Daniel, K.L. Cavalca, Dynamic analysis of a lubricated planar slider–crank mechanism considering friction and Hertz contact effects, Mechanism and Machine Theory, 74 (2014) 257-273.

[10] M. Machado, J. Costa, E. Seabra, P. Flores, The effect of the lubricated revolute joint parameters and hydrodynamic force models on the dynamic response of planar multibody systems, Nonlinear Dynamics, 69 (2012) 635-654.

[11] C. Brutti, G. Coglitore, P.P. Valentini, Modeling 3D revolute joint with clearance and contact stiffness, Nonlinear Dynamics, 66 (2011) 531-548.

[12] I. Khemili, L. Romdhane, Dynamic analysis of a flexible slider–crank mechanism with clearance, European Journal of Mechanics-A/Solids, 27 (2008) 882-898.

[13] S. Mukras, N.H. Kim, N.A. Mauntler, T.L. Schmitz, W.G. Sawyer, Analysis of planar multibody systems with revolute joint wear, Wear, 268 (2010) 643-652.

[14] Z. Zhang, L. Xu, Y.Y. Tay, P. Flores, H. Lankarani, Multi-objective optimization of mechanisms with clearances in revolute joints, in: New Trends in Mechanism and Machine Science, Springer, 2015, pp. 423-433.

[15] S.M. Varedi, H.M. Daniali, M. Dardel, A. Fathi, Optimal dynamic design of a planar slider-crank mechanism with a joint clearance, Mechanism and Machine Theory, 86 (2015) 191-200.

[16] A. Sardashti, H.M. Daniali, S.M. Varedi, Optimal free-defect synthesis of four-bar linkage with joint clearance using PSO algorithm, Meccanica, 48 (2013) 1681-1693.

[17] S. Erkaya, I. Uzmay, A neural–genetic (NN–GA) approach for optimising mechanisms having joints with clearance, Multibody System Dynamics, 20 (2008) 69-83.

[18] S. Rahmanian, M.R. Ghazavi, Bifurcation in planar slider–crank mechanism with revolute clearance joint, Mechanism and Machine Theory, 91 (2015) 86-101.

[19] J. Chunmei, Q. Yang, F. Ling, Z. Ling, The non-linear dynamic behavior of an elastic linkage mechanism with clearances, Journal of Sound and Vibration, 249 (2002) 213-226.

[20] A.M. Vaidya, P.M. Padole, A performance evaluation of four bar mechanism considering flexibility of links and joints stiffness, Open Mechanical Engineering Journal, 4 (2010) 16-21.

[21] S. Erkaya, Prediction of vibration characteristics of a planar mechanism having imperfect joints using neural network, Journal of Mechanical Science and Technology, 26 (2012) 1419-1430.

[22] G. Yang, J. Yang, C. Qiang, J. Ge, Q. Chen, Natural frequencies of a cantilever beam and block system with clearance while block staying on given position, Journal of Vibration and Control, 19 (2013) 262-275.

[23] E. Salahshoor, S. Ebrahimi, M. Maasoomi, Nonlinear vibration analysis of mechanical systems with multiple joint clearances using the method of multiple scales, Mechanism and Machine Theory, 105 (2016) 495-509.

[24] P. Flores, H.M. Lankarani, Contact force models for multibody dynamics, Springer International Publishing, 2016.

[25] P. Flores, Dynamic analysis of mechanical systems with imperfect kinematic joints, in, University of Minho, Braga, Portugal, 2004.

[26] J.K. Kevorkian, J.D. Cole, Multiple scale and singular perturbation methods, Springer-Verlag New York, 1996.

[27] A.H. Nayfeh, D.T. Mook, Nonlinear oscillations, John Wiley & Sons, 1995.

[28] A.F. El-Bassiouny, Structural modal interactions with internal resonances and external excitation, Physica Scripta, 72 (2005) 132-141.

[29] R.J. Schiling, S.L. Harris, Applied numerical methods for engineers using MATLAB, Brooks/Cole Publishing Co., Pacific Grove, CA, USA, 2000.